machines

MDPI

Article

Semi-Active Suspension Design for an In-Wheel-Motor-Driven Electric Vehicle Using a Dynamic Vibration-Absorbing Structure and PID-Controlled Magnetorheological Damper

Kyle Samaroo, Abdul Waheed Awan * and Sheikh Islam

Department of Engineering, University of Staffordshire, College Road, Stoke on Trent ST4 2DE, UK; kyle.samaroo@staffs.ac.uk (K.S.); sheikh.islam@staffs.ac.uk (S.I.)
* Correspondence: a.awan@staffs.ac.uk

Abstract: The in-wheel motor (IWM) powertrain layout offers greater design flexibility and higher efficiency of an electric vehicle but has limited commercial success mainly due to the concerns of increased unsprung mass. This paper proposes a semi-active suspension system for in-wheel motors that combines both a dynamic vibration-absorbing structure (DVAS) and a PID-controlled MR damper, in order to achieve optimised comfort, handling and IWM vibration for a small car application. Whilst PID control and DVAS are not entirely new concepts, the usage of both optimisation techniques in a semi-active in-wheel motor suspension has seen limited implementation, which makes the current work novel and significant. The semi-active suspension operating both in passive fail-safe mode and full feedback control was compared to a conventional in-wheel motor passive suspension in terms of sprung mass acceleration, displacement, stator acceleration, tyre deflection and suspension travel for three different road profile inputs using MATLAB/Simulink. The implementation of a PID-controlled MR damper improved road comfort and road holding performance and decreased in-wheel motor vibration over the DVAS passive suspension mainly in terms of a maximum peak amplitude decrease of 40%, 35% and 32% for the sprung mass acceleration, tyre deflection and stator acceleration, respectively. The results are significant since they show that the use of a simple, easily implemented control scheme like PID control was able to significantly improve IWM suspension performance when paired with a DVAS. This study provides further confidence to manufacturers to commercially develop and implement the IWM layout as its major disadvantage can be reasonably addressed using a simple readily available control approach.

Keywords: in-wheel motor; semi-active suspension; DVAS; PID; Bouc-Wen; MR damper; MATLAB/Simulink

Academic Editors: Yumeng Yao, Yuming Yin, Zhijun Fu and Subhash Rakheja

Received: 6 December 2024
Revised: 5 January 2025
Accepted: 8 January 2025
Published: 11 January 2025

Citation: Samaroo, K.; Awan, A.W.; Islam, S. Semi-Active Suspension Design for an In-Wheel-Motor-Driven Electric Vehicle Using a Dynamic Vibration-Absorbing Structure and PID-Controlled Magnetorheological Damper. *Machines* **2025**, *13*, 47. https://doi.org/10.3390/machines13010047

1. Introduction

In light of the 2015 Paris agreement, significant efforts are being made to decarbonise the road transportation sector whereby electrification is regarded as the most viable solution [1]. Whilst electric vehicles (EVs) are becoming more popular, the associated technology is still in constant development, and currently, many OEMs (original equipment manufacturers) still produce consumer light electric vehicles (LEVs) based on the traditional centralised motor powertrain layout based on the internal combustion engine (ICE) vehicles of existing design. However, the inherent differences between an EV and an ICE vehicle mean that the centralised motor is not the ideal or most appropriate powertrain layout [2].

The in-wheel motor (IWM) layout is an alternative which can provide significant benefits when used in an EV. Compared to a centralised motor, the IWM layout allows better dynamic control and higher efficiency since each wheel is powered independently and directly without the need for a mechanical transmission system [3]. Furthermore, the IWM layout is more compact which allows greater flexibility in terms of weight and space saving or even for the addition of range extender engines or more batteries to increase range [4,5]. Despite its advantages, there has been a lack of commercial adoption of the IWM layout, mainly due to the fact that installing the electric motors inside the wheels leads to an increased unsprung mass of the vehicle's suspension which, in turn, can severely deteriorate ride comfort and road holding (handling) performance [5]. The extent to which unsprung mass affects the suspension performance has been a popular and controversial research topic. Kulkarni et al. [6] compared the dynamic suspension performance of a standard internal combustion engine (ICE) vehicle to an in-wheel switched reluctance motor (SRM) EV, using a three-degrees-of-freedom quarter car model. It was found that the in-wheel SRM EV had a noticeable deterioration of ride comfort and road handling performance based on an amplitude increase of 15–25% in terms of the velocity and displacement response plots of the in-wheel SRM EV as compared to the standard ICE vehicle. A more in-depth analysis of the ride comfort of in-wheel motor EVs was presented by Jin et al. [7]. In this case, an 11-degrees-of-freedom full car model was used to compare the suspension performance between a standard vehicle and one with an added 30 kg of unsprung mass. Overall, Jin et al. [7] found that there was a substantial decrease in ride comfort performance mainly due to a significant increase in the dynamic tyre load of the suspension system with the added unsprung mass. However, Anderson and Harty [8] presented a comprehensive analysis of the impact of increased unsprung mass on dynamic suspension performance based on a number of indicators which included objective measurements, subjective assessment and predictive analysis. This was a collaborate research conducted by Lotus Engineering and Dunamos Ltd., where both experimental and simulation methods (MATLAB/Simulink) were utilised. In terms of ride comfort, it was noted that there were indeed perceptible differences due to the increased unsprung mass, but overall, the differences were small, and it was unlikely that the degraded performance would largely affect or be noticed by the average driver. Regardless, unsprung mass is often the most quoted drawback of the IWM in both academia and industry, as highlighted by [9].

Moreover, there are other notable concerns of the IWM layout such as the lifespan and fatigue of the in-wheel motor due to the direct impact of road vibrations [5,9]. Kulkarni et al. [10] investigated the fatigue and lifecycle of an in-wheel SRM EV suspension with increased unsprung mass using Finite Element Analysis (FEA). In this case, the in-wheel SRM suspension was subjected to variable amplitude fatigue and the overall suspension system was proven to be safe as total in-wheel SRM suspension life was calculated as 208,800 miles. Additionally, Kulkarni and Kapoor [11] designed and tested various rim designs for housing an in-wheel SRM using FEA software (ANSYS Workbench 13.1). When evaluated in terms of structural integrity, thermal stability and life cycle assessment, a two-piece hollow end-cap rim design of 7 kg was optimal in housing the in-wheel SRM.

As such, further optimisation of the in-wheel motor suspension system is highly desirable in order to realise greater ride performance and durability, which can improve the commercial uptake of the in-wheel motor layout. Two promising optimisation techniques are the implementation of controllable semi-active or active devices and the use of a dynamic vibration-absorbing structure (DVAS) in the suspension in order to suppress the negative effects of the increased unsprung mass [3].

Semi-active suspensions have been favoured commercially by automotive OEMs since the 1990s due to its ability to offer the best compromise of cost (in terms of power consump-

tion, weight, sensor requirement) and performance (comfort and handling) as compared to the active suspension [12]. Also, the semi-active suspension is a safer alternative to the active counterpart since the system can operate in passive fail-safe mode if the control system fails and power cannot be delivered to the semi-active damper [13]. In order to facilitate semi-active damping control, various actuator options are available including servo/solenoid dampers, magnetorheological (MR)/electrorheological (ER) dampers and electromagnetic dampers. However, commercially available semi-active dampers typically use MR/ER fluids due to the technological advantages and cost efficiency [12]. These fluids are a class of smart materials whose rheological properties (viscosity and yield stress) can be adjusted based on the intensity of the respective magnetic or electric field which is applied [14]. Furthermore, it was eventually found that MR fluids were better suited to most applications (like suspensions) since MR fluids experience a much greater increase in viscosity and yield strength compared to ER fluids [15]. MR fluids consist of micron-sized, magnetisable particles suspended in a carrier medium such as mineral or silicone oil. When a magnetic field is applied to the fluids (via a current or voltage command), particle chains are formed, and the fluid changes from being viscous free-flowing to a semi-solid state in milliseconds, therefore developing the required damping force. The MagneRide suspension system developed by Delphi Automotive Systems is based on MR damper technology, and it has been used commercially by OEMs such as Cadillac, Chevrolet and Land Rover since the 2000s [12].

It follows that there now exists rich literature surrounding semi-active and active suspension systems where researchers have used various control methods and modelling techniques to continuously improve suspension performance. Sun et al. [16] proposed an (ARC)-based H-Infinity controller for an active suspension system in order to mitigate vibration and improve ride comfort. A full car model was developed, and the active suspension was modelled with electrohydraulic actuators that had highly non-linear characteristics. The proposed active suspension with ARC-based H-Infinity control significantly improved ride comfort performance over a passive suspension and also compared to other popular control variations, namely a backstepping-based H-Infinity controller [16]. Agharkakli et al. [17] designed an LQR-controlled active quarter car suspension without actuator dynamics. The proposed LQR-controlled active suspension improved ride comfort over the passive suspension in terms of lower amplitudes and faster settling time of the various response plots.

Rashid et al. [18] investigated the performance of different control strategies used in a semi-active suspension system (PID, fuzzy logic and fuzzy-hybrid) in order to improve ride comfort and handling. The semi-active suspension was implemented with a controllable MR damper which was modelled using the voltage-dependent modified Bouc-Wen parametric model. In general, it was found that a semi-active suspension implemented with a controllable MR damper can effectively improve ride comfort and vehicle handling where the fuzzy and fuzzy-hybrid controller's performance was noticeably better than that of the PID controller.

DVAS is another viable optimisation technique to suppress the negative effects of the increased unsprung mass due to the in-wheel motor location in the suspension system. In a conventional electric wheel, the motor (rotor and stator) is rigidly connected to the tyre, rim and wheel axle resulting in the undesirable increase in unsprung mass [3]. Additionally, road excitations are directly transferred to the in-wheel motor resulting in reduced motor lifespan. However, when using a DVAS, the in-wheel motor is flexibly connected and suspended by extra springs or dampers, resulting in improved suspension performance. The DVAS can be implemented in terms of a 'tyre' type in which the in-wheel motor

is flexibly connected to the wheel axle or with the 'chassis' type wherein the motor is connected to the sprung mass [19].

The current literature on DVAS optimisation technique is quite limited, and only a few researchers have carried out simulated or experimental testing. Qin et al. [19] presented an analysis of the various DVAS designs used to mitigate vibration for EVs with in-wheel switch reluctance motors (SRMs). The two main DVAS layouts, i.e., 'tyre' type and 'chassis' type, were simulated and tested under different road grades at varying vehicle speeds. It was concluded that the extra unsprung mass of an in-wheel SRM does indeed deteriorate performance but the implementation of either a 'chassis or 'tyre' type DVAS can negate the effects of the increased unsprung mass, with proper system parameter optimisation. Specifically, the 'tyre' type DVAS offered slightly better performance than the 'chassis' type in terms of ride comfort and road holding and was overall a much more feasible design for mass-produced vehicles.

Moreover, researchers have chosen to combine both optimisation techniques, i.e., control strategies and DVAS, in order to realise further improvements in terms of IWM suspension performance. Qin et al. [20] presented a hybrid (sky-hook–ground-hook) control strategy for an IWM EV suspension system, to improve ride comfort and IWM vibration. In this case, an MR damper was used as the controllable semi-active actuator wherein the damper force was obtained via real-life experimental testing using an MTS test rig, unlike the use of models such as the Bouc-Wen MR damper model. Two disturbance inputs (random road excitation in frequency domain and bump input in time domain) were used to generate the system responses. Ride comfort, road holding performance and IWM vibration were assessed based on sprung mass acceleration, tyre deflection system response and stator mass acceleration of the IWM, respectively. It was concluded that the hybrid control strategy paired with a DVAS can improve ride comfort, road holding and, more importantly, extend IWM lifespan (by reduction in IWM vibration) compared to the IWM suspension system with just a DVAS and compared to a standard passive setup [20]. Xu et al. [5] proposed and validated a novel hybrid-ADD (acceleration driven damping) control strategy for use in a DVAS-based semi-active IWM suspension to improve ride comfort and reduce IWM vibration. The motor dynamics (including unbalanced electromagnetic force induced by the IWM) were modelled and the MR damper force characteristics were replicated in simulation based on experimental testing. Xu et al. [5] concluded that the inclusion of a DVAS can improve both ride comfort and IWM vibration compared to the IWM suspension without a DVAS. The proposed hybrid-ADD control strategy can then further improve performance of the standard DVAS. Zhang et al. [21] designed and simulated an in-wheel motor suspension which used both a DVAS as well as a tandem inerter spring damper device (ISD). An improved sky-hook controller was implemented, which uses body vertical velocity as the basis for damping adjustment. It was found that the combination of ISD suspension and DVAS improved ride comfort by 27.6% and the sky-hook control offered further improvements. Notably, the sky-hook controller improved suspension working space at low frequencies whilst worsening the resonance peak at higher frequencies. In [22], a dual-loop active suspension control system based on particle swarm optimisation and PID control was proposed for an in-wheel motor electric vehicle. Tan et al. [22] considered vertical excitations from the road vibrations and unbalanced electromagnetic force produced by motor magnet gap deformation. The PID gains of the controller were selected using the particle swarm optimisation method as opposed to user adjustment. An improvement of 20.92% was obtained in vertical vibration acceleration compared to the standard passive suspension. Xu et al. [23] designed and validated a DVAS-based electrohydraulic active suspension for an in-wheel motor vehicle. The DVAS used an actuator between the sprung and unsprung mass to create active force, which

was then controlled using a sky-hook controller. It was found that a sky-hook coefficient approaching 5000 produced a good compromise between road comfort and handling. Xu et al. [23] also clarified values for hydraulic pressure of the active system based on experimental testing, where the largest experimental error between experimental and numerical hydraulic pressure was 18.8%.

This paper further advances the objective of IWM optimisation by designing and modelling a DVAS-based semi-active suspension which uses a PID-controlled Bouc-Wen MR damper to achieve optimised comfort and handling and reduced IWM vibration of a small IWM-driven car application. A multi-degree-of-freedom, lumped-element quarter car model is constructed in MATLAB/Simulink, and a variety of road profiles/conditions are used to thoroughly assess and investigate the suspension performance.

Whilst the use of DVAS and PID control as separate entities are not entirely new, the implementation of both DVAS and PID control for a semi-active suspension of an in-wheel motor vehicle has not been yet been researched, to the authors' best knowledge. Other researchers [5,20,21,23] have instead chosen to implement different control strategies such as sky-hook, ground-hook or novel hybrids in conjunction with the DVAS for an IWM-driven vehicle. Furthermore, when PID control was implemented for an IWM vehicle in [22], this was carried out for an active suspension setup without the use of DVAS. PID control is an attractive option since it is the most widespread type of closed-loop controller used in the industry and can be implemented with little prior knowledge of the system [24], which are notable implications for furthering commercial uptake of the IWM layout. Furthermore, a semi-active suspension based on the MR damper was used in the current work since it is widely preferred by automotive OEMs due to performance and cost and has seen large commercial implementation. Additionally, this paper has further novelty since the response of the semi-active suspension in passive fail-safe mode was investigated, which has not been carried out in previous work.

2. Materials and Methods

2.1. Suspension Performance Criteria

A suspension performance criteria or objectives were derived to assess the response of the suspension systems tested. They may be stated as follows:

Minimise:

1. sprung mass acceleration, $\ddot{x_1}$
2. sprung mass displacement, x_1
3. stator acceleration, $\ddot{x_s}$
4. tyre deflection, $(x_2 - w)$

Subject to:

5. Suspension travel limits, $(x_1 - x_2)$

In the minimisation problem, $\ddot{x_1}$ and x_1 measures ride comfort, $\ddot{x_s}$ measures IWM vibrations, and $(x_2 - w)$ measures road holding. Due to variations in vehicle application and design, exact suspension travel limits were not defined, but instead, the suspension travel response was simply analysed. However, as a general guideline, Gillespie [25] notes that small, compact cars typically have a suspension stroke or travel of 5 to 6 inches (i.e., 0.127 m to 0.152 m).

2.2. Road Profile Modelling

Three road profiles were selected and modelled in MATLAB/Simulink for suspension testing in the time domain. These profiles were selected based on typical disturbances a vehicle might face in a real-life scenario. Figures 1–3 show the respective road profile traces.

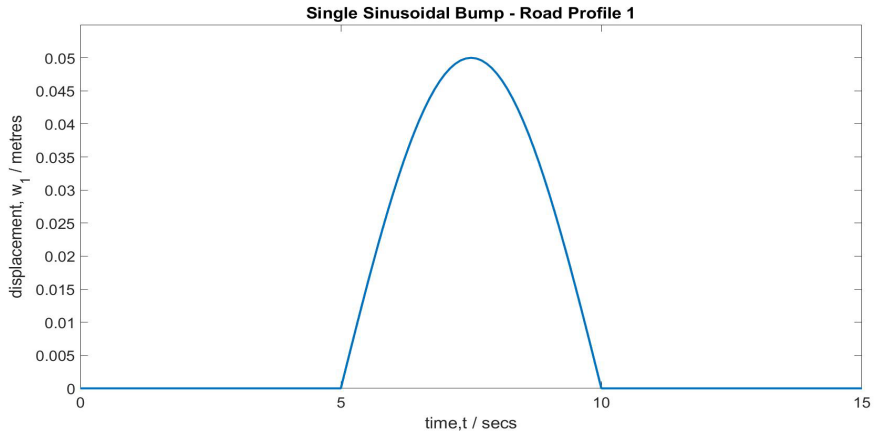

Figure 1. A 0.1 Hz single sinusoidal bump profile defined by equation $w_1(t)$.

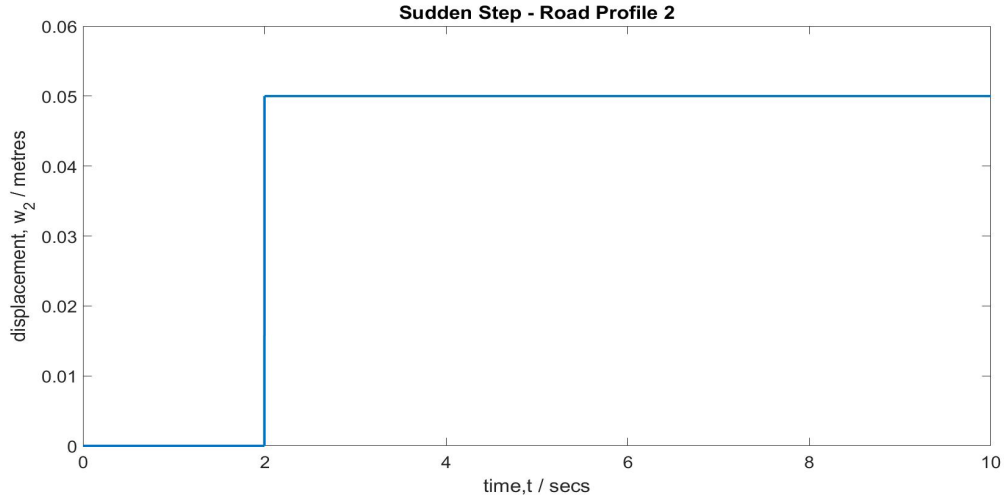

Figure 2. A 0.05 m sudden step road profile defined by equation $w_2(t)$.

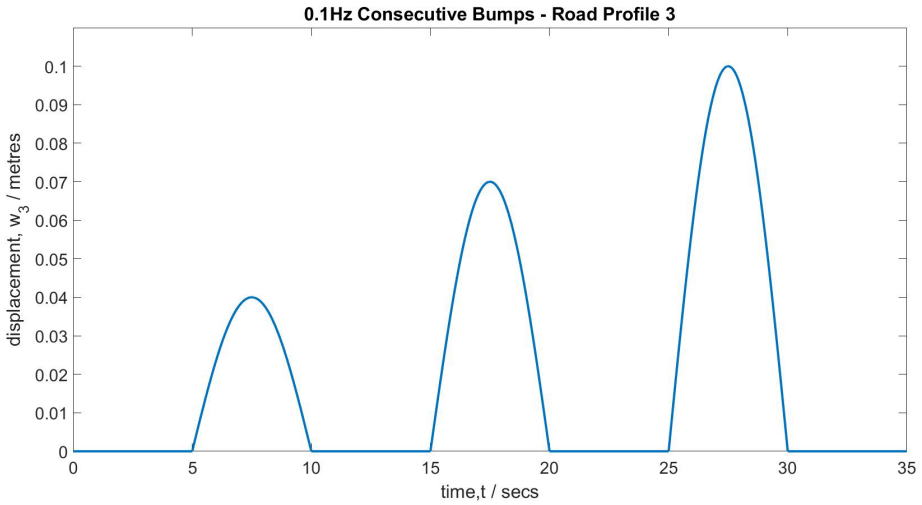

Figure 3. A 0.1 Hz consecutive bumps profile defined by equation $w_3(t)$.

6. Road Profile 1—0.1 Hz single sinusoidal bump

$$w_1(t) = \begin{matrix} -0.05\sin(0.2\pi t) & 5\text{ s} \le t \le 10\text{ s} \\ 0\text{ m} & \textit{otherwise} \end{matrix}$$

7. Road Profile 2—0.05 m sudden step

$$w_2(t) = \begin{matrix} 0 & 0\,\text{s} \le t < 2\,\text{s} \\ 0.05\,\text{m} & t \ge 2\,\text{s} \end{matrix}$$

8. Road Profile 3—0.1 Hz consecutive bumps of increasing amplitude

$$w_3(t) = \begin{cases} -0.04sin(0.2\pi t)\ 5\ s \le t \le 10\ s \\ -0.07sin(0.2\pi t)\ 15\ s \le t \le 20\ s \\ -0.1sin(0.2\pi t)\ 25\ s \le t \le 30\ s \\ 0\ otherwise \end{cases}$$

2.3. Conventional IWM Passive Suspension System (CON IWM-PSS): Mathematical Modelling

The conventional IWM passive suspension system (i.e., without semi-active control or DVAS) was firstly modelled based on the quarter car model shown in Figure 4 below. In Figure 4, it can be seen that the conventional passive suspension is modelled with a lumped unsprung mass, m_{2con}, which includes both the IWM (rotor and stator) mass as well as the other typical unsprung suspension components.

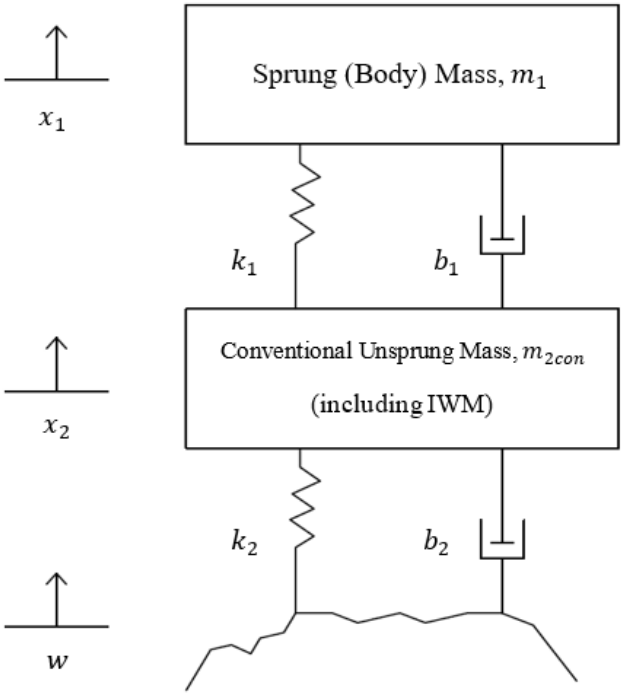

Figure 4. Conventional passive suspension quarter car diagram.

Sprung (body) mass equation of motion:
Using Newton' 2nd law, $\sum F = ma$,

$$-k_1(x_1 - x_2) - b_1(\dot{x_1} - \dot{x_2}) = m_1(\ddot{x_1}) \quad (1)$$

Unsprung (suspension) mass equation of motion:

$$-k_2(x_2 - w) - b_2(\dot{x_2} - \dot{w}) + k_1(x_1 - x_2) + b_1\left(\dot{x_1} - \dot{x_2}\right) = m_{2con}(\ddot{x_2}) \quad (2)$$

2.4. Conventional IWM Passive Suspension System (CON IWM-PSS): Simulink Modelling

Figure 5 below shows the conventional passive suspension model constructed in a MATLAB/Simulink environment.

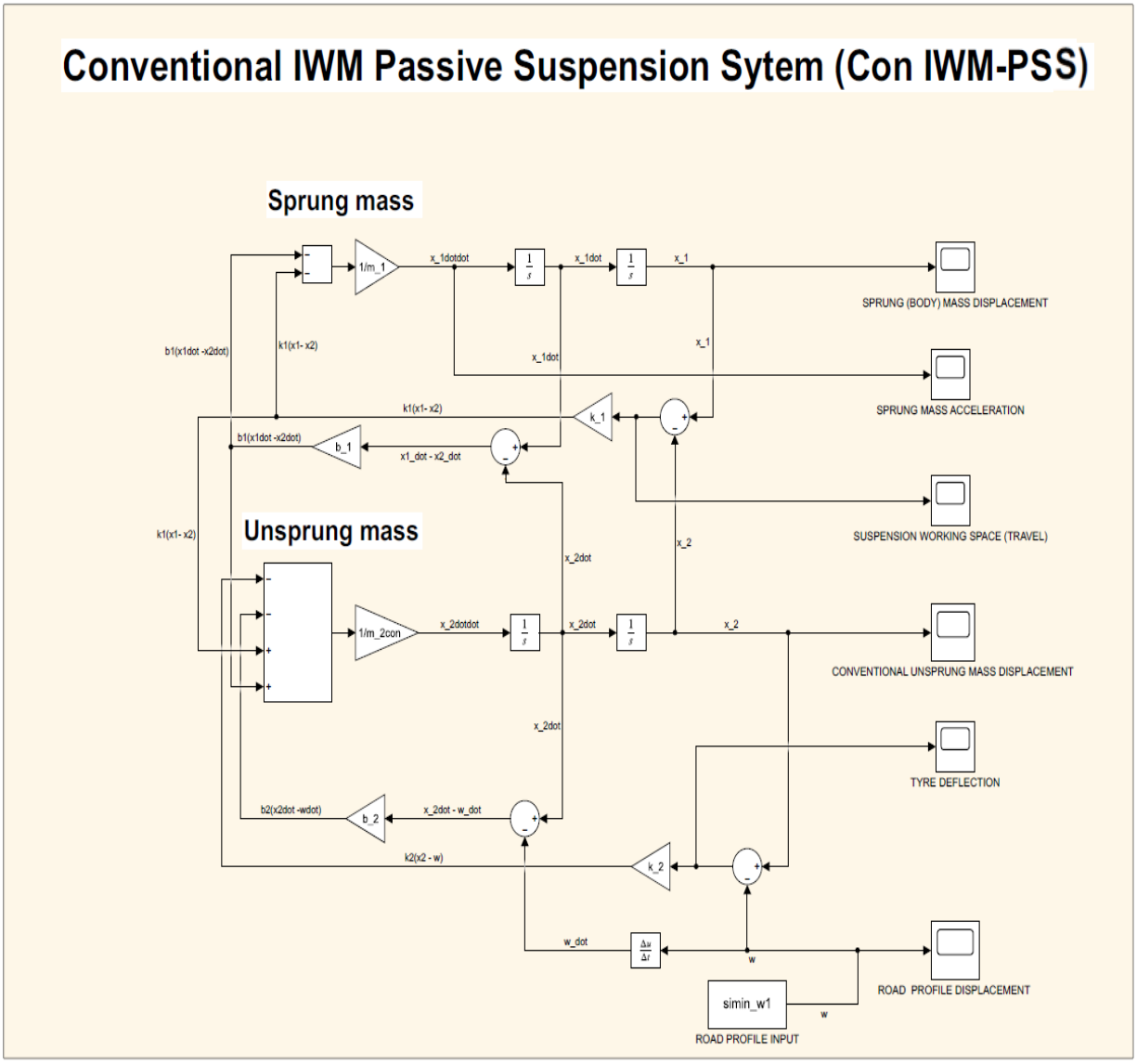

Figure 5. Simulink model of conventional passive suspension quarter car model.

Table 1 outlines the system parameter values that were chosen for use in the simulation of the conventional passive suspension, where the values were based on [26].

Table 1. Suspension system parameters considered for quarter car modelling of conventional passive suspension.

Parameter	Value
m_1	450 kg
m_{2con}	68 kg
k_1	28,500 N/m
k_2	293,900 N/m
b_1	2700 Ns/m
b_2	0 Ns/m

2.5. DVAS-Based IWM Passive Suspension System (DVAS IWM-PSS) Mathematical Modelling

Figure 6 shows the DVAS-based IWM passive suspension system wherein the rotor mass and stator mass of the IWM, m_r and m_s are supported by an additional damper, spring and bearing which constitute the DVAS.

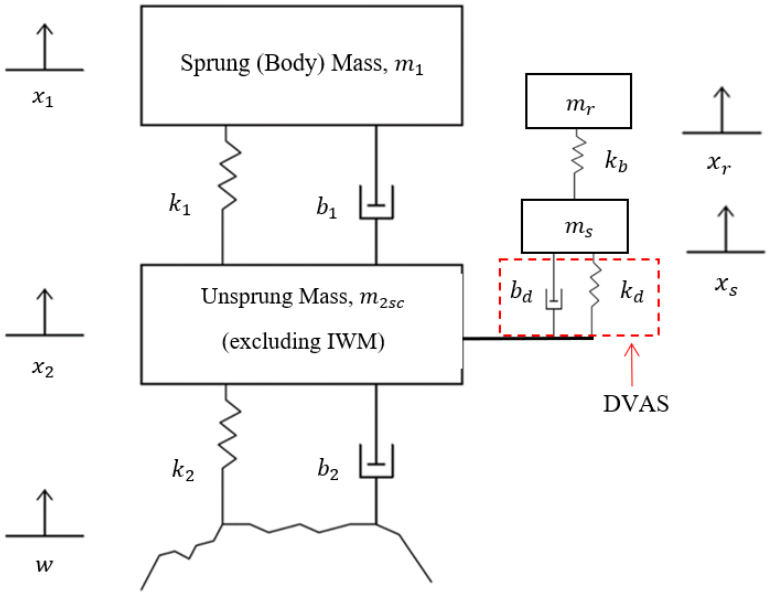

Figure 6. DVAS-based IWM passive suspension diagram.

The time domain equations of the DVAS passive suspension system were derived based on the quarter car suspension diagram in Figure 6.

Sprung (body) mass equation of motion:

Using Newton' 2nd law, $\sum F = ma$,

$$m_1(\ddot{x_1}) = -k_1(x_1 - x_2) - b_1(\dot{x_1} - \dot{x_2}) \tag{3}$$

Unsprung (suspension) mass equation of motion:

$$m_2(\ddot{x_2}) = -k_2(x_2 - w) - b_2(\dot{x_2} - \dot{w}) + k_1(x_1 - x_2) + b_1\left(\dot{x_1} - \dot{x_2}\right) + k_d(x_s - x_2) + b_d\left(\dot{x_s} - \dot{x_2}\right) \tag{4}$$

Stator mass equation of motion:

$$m_s(\ddot{x_s}) = -k_d(x_s - x_2) - b_d(\dot{x_s} - \dot{x_2}) + k_b(x_r - x_s) \tag{5}$$

Rotor mass equation of motion:

$$m_r(\ddot{x_r}) = -k_b(x_r - x_s) \tag{6}$$

2.6. DVAS-Based IWM Passice Suspension System (DVAS IWM-PSS): Simulink Modelling

Figure 7 shows the DVAS-based passive suspension model constructed in a MATLAB/Simulink environment based on the equations derived.

Table 2 outlines the system parameter values that were chosen for use in the simulation of the DVAS passive suspension system. All suspension parameters used in the conventional passive suspension were retained, and any additional parameters unique to the DVAS such as damping coefficient of DVAS damper (b_d), stiffness of DVAS spring (k_d) and bearing stiffness (k_b) were based on the parametrization carried out by [5].

It should be noted that the sum of the unsprung (suspension components) mass, stator mass and rotor mass (m_{2sc}, m_s and m_r, respectively) in the DVAS IWM-PSS was equal to the conventional unsprung mass, m_{2con} of the CON IWM-PSS, i.e., ($m_{2con} = m_{2sc} + m_s + m_r$).

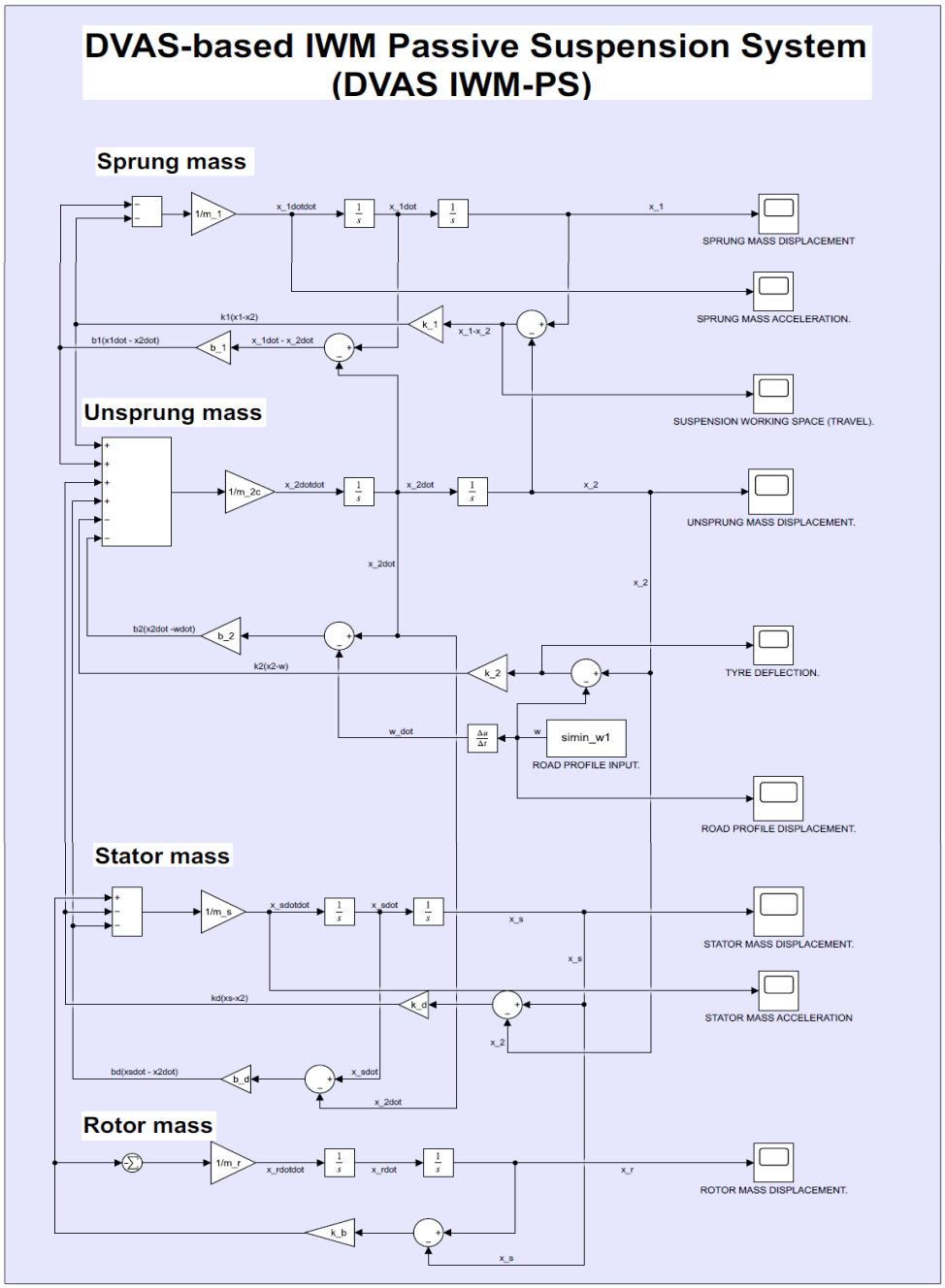

Figure 7. Simulink model of the DVAS-based passive suspension system.

Table 2. System parameter values used in the DVAS IWM-PSS.

Parameter	Value
m_1	450 kg
m_{2sc}	23 kg
m_s	20 kg
m_r	25 kg
k_1	28,500 N/m
k_2	293,900 N/m
b_1	2700 Ns/m
b_2	0 Ns/m
b_d	1900 Ns/m
k_d	53,000 N/m
k_b	1.4×10^7 N/m

2.7. DVAS-Based IWM Semi-Active Suspension System (DVAS IWM-SASS): Mathematical Modelling

The DVAS-based IWM semi-active suspension system was implemented using an MR damper represented via the Bouc-Wen hysteretic model. The Bouc-Wen model efficiently represents the MR damper's non-linear dynamics.

The time domain equations of the DVAS IWM-SASS were derived based on quarter car semi-active suspension diagram shown in Figure 8.

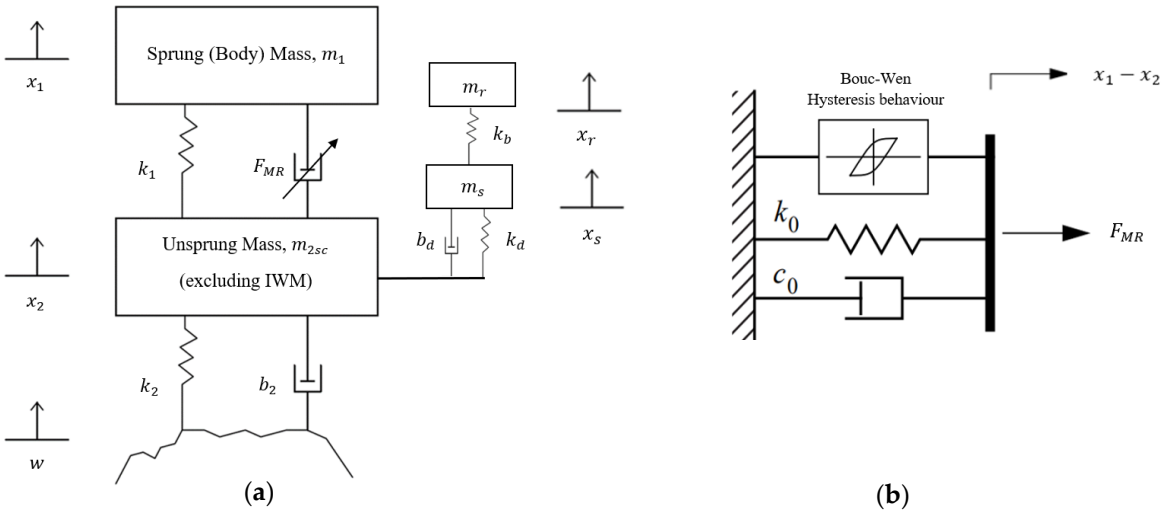

Figure 8. (**a**) DVAS IWM-SASS quarter car suspension diagram; (**b**) Bouc-Wen (BW) model of controllable semi-active MR damper.

Sprung (body) mass equation of motion:
Using Newton' 2nd law, $\sum F = ma$,

$$m_1(\ddot{x_1}) = -k_1(x_1 - x_2) - F_{MR} \tag{7}$$

Unsprung (suspension) mass equation of motion:

$$m_2(\ddot{x_2}) = -k_2(x_2 - w) - b_2(\dot{x_2} - \dot{w}) + k_1(x_1 - x_2) + F_{MR} + k_d(x_s - x_2) + b_d\left(\dot{x_s} - \dot{x_2}\right) \tag{8}$$

Stator mass equation of motion:

$$m_s(\ddot{x_s}) = -k_d(x_s - x_2) - b_d(\dot{x_s} - \dot{x_2}) + k_b(x_r - x_s) \tag{9}$$

Rotor mass equation of motion:

$$m_r(\ddot{x_r}) = -k_b(x_r - x_s) \tag{10}$$

Standard (constant zero voltage) Bouc-Wen MR damper model:

$$F_{MR} = k_0((x_1 - x_2) - x_0) + c_0(\dot{x_1} - \dot{x_2}) + \alpha z \tag{11}$$

Evolutionary variable, z, is given by

$$\dot{z} = -\gamma|\dot{x_1} - \dot{x_2}|z|z|^{n-1} - \beta\dot{x}|z|^n + A(\dot{x_1} - \dot{x_2}) \tag{12}$$

Voltage-dependent Bouc-Wen MR damper model:

In order to implement a controllable MR damper, the standard Bouc-Wen damper model was further generalised to account for fluctuating applied voltage (v) and hence magnetic field.

$$\alpha = \alpha(u) = \alpha_a + \alpha_b(u) \tag{13}$$

$$c_0 = c_0(u) = c_{0a} + c_{0b}(u) \tag{14}$$

$$\dot{u} = -\eta(u - v) \tag{15}$$

2.8. DVAS-Based IWM Semi-Active Suspension System (DVAS IWM-SASS): Control Strategy

Figure 9 shows the closed feedback loop of the DVAS semi-active suspension in which the PID controller was employed.

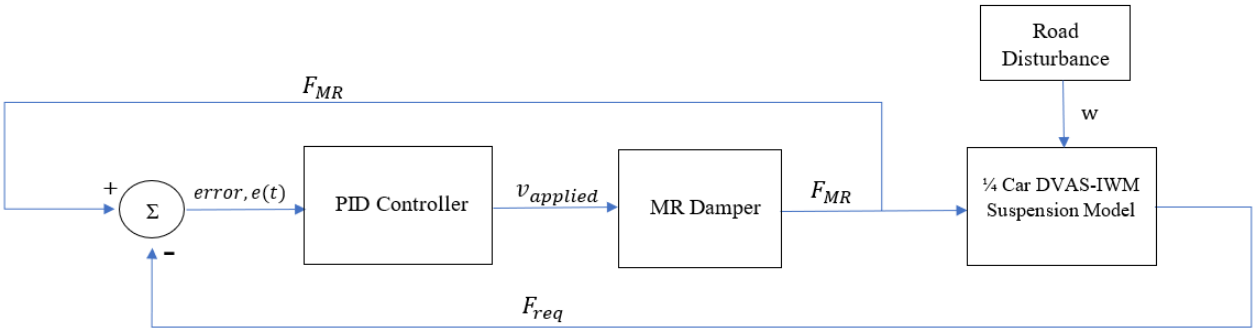

Figure 9. Block diagram of the control scheme for the DVAS semi-active suspension.

An overview of the PID controller schematic is shown in Figure 10. The error, $e(t)$, represents the controller input and is given as the difference between the output damping force of the MR damper, F_{MR}, and a reference value which is the required damping force of the system (F_{req}). In this case, F_{req} is taken as the total force experienced by the sprung mass, i.e., $(m_1\ddot{x}_1)$.

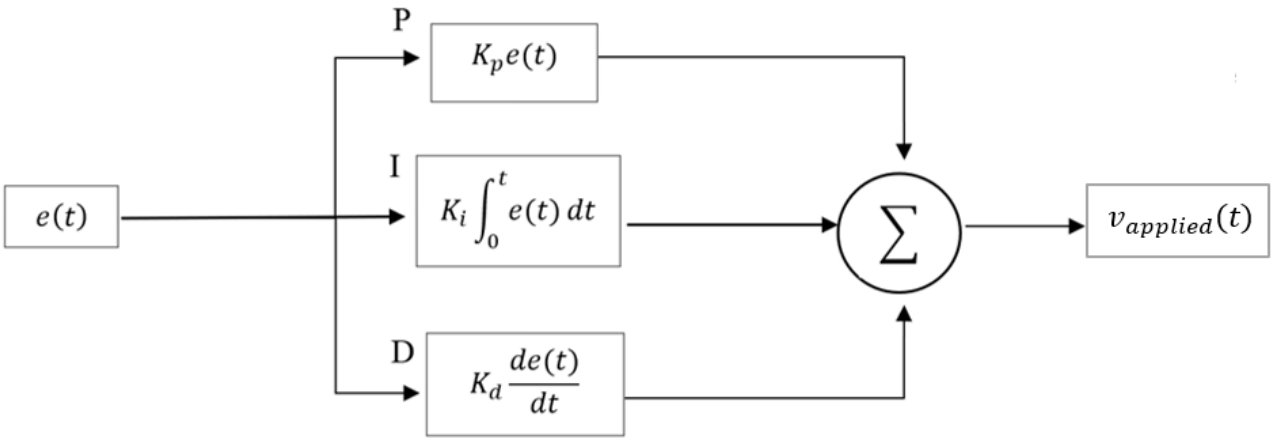

Figure 10. Schematic of the PID controller used in the control scheme of the DVAS IWM-SASS.

Mathematically, the error term is expressed as follows:

$$e(t) = F_{MR} - F_{req} \tag{16}$$

$$e(t) = F_{MR} - m_1\ddot{x}_1 \tag{17}$$

The subsequent control output, $v_{applied}(t)$, of the PID controller in the DVAS IWM-SASS is given by

$$v_{applied}(t) = K_p e(t) + K_i \int_0^t e(t)dt + K_d \frac{de(t)}{dt} \quad (18)$$

As seen in Equation (18), the PID controller algorithm involves the weighted sum of three separate, constant parameters, which are the proportional (K_p), integral (K_i) and derivative (K_d) gain. Each of these gains are a tuning parameter which must be selected appropriately to achieved the desired system performance.

Based on the error control input supplied, the PID controller provides the required voltage, $v_{applied}(t)$, to the MR damper such that damping force of the MR damper tracks the reference damping force, (F_{req}), and the error term is therefore minimised. In this way, the closed-loop feedback PID controller is able to select the applied voltage, $v_{applied}(t)$, and hence the MR damper force, F_{MR}, which is required for the particular road profile experienced.

2.9. DVAS-Based IWM Semi-Active Suspension System (DVAS IWM-SASS): Simulink Modelling

In the Simulink environment, the DVAS semi-active suspension was implemented based on the equations derived for the voltage-dependent Bouc-Wen MR damper model and PID controller. Figure 11 shows the Simulink block diagram of the overall DVAS semi-active suspension. Figure 12 then shows the DVAS semi-active subsystem, whilst Figure 13a presents the PID controller subsystem, and Figure 13b displays the Bouc-Wen MR damper subsystem in Simulink.

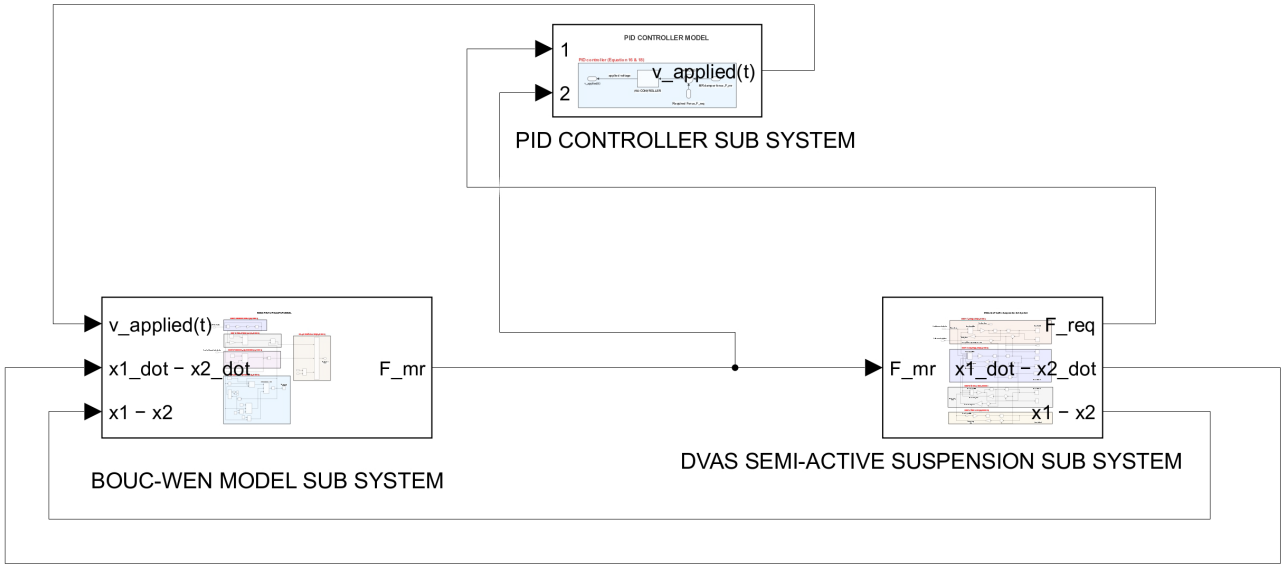

Figure 11. Simulink block diagram of the overall DVAS semi-active suspension.

In order to implement the Bouc-Wen model, suitable values need to be chosen for the variables of the Bouc-Wen equations to model the real-life dynamics of an MR damper. The identification of the hysteresis loop parameters is quite complex and often requires extensive experimental testing and numerical studies. As this was not the main focus of the current work, the initial parametrisation of the Bouc-Wen model was based on the values used in [26]. Table 3 outlines the initial parameters of the Bouc-Wen MR damper model that were chosen for use in the simulation of the DVAS semi-active suspension system. All other suspension parameters that were consistent with the prior DVAS passive suspension were retained in the simulation of the DVAS semi-active suspension.

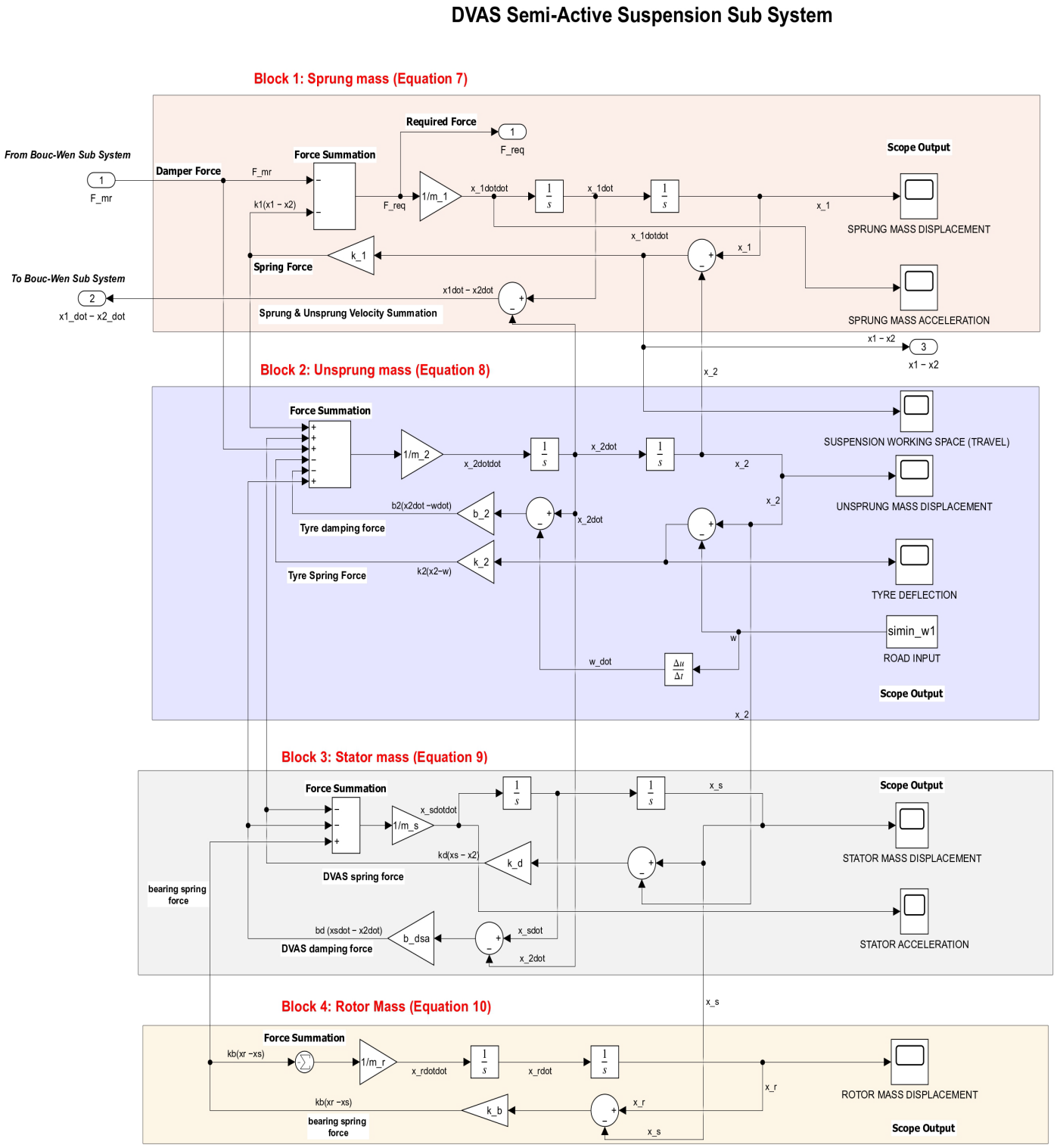

Figure 12. Simulink model of the DVAS semi-active suspension subsystem.

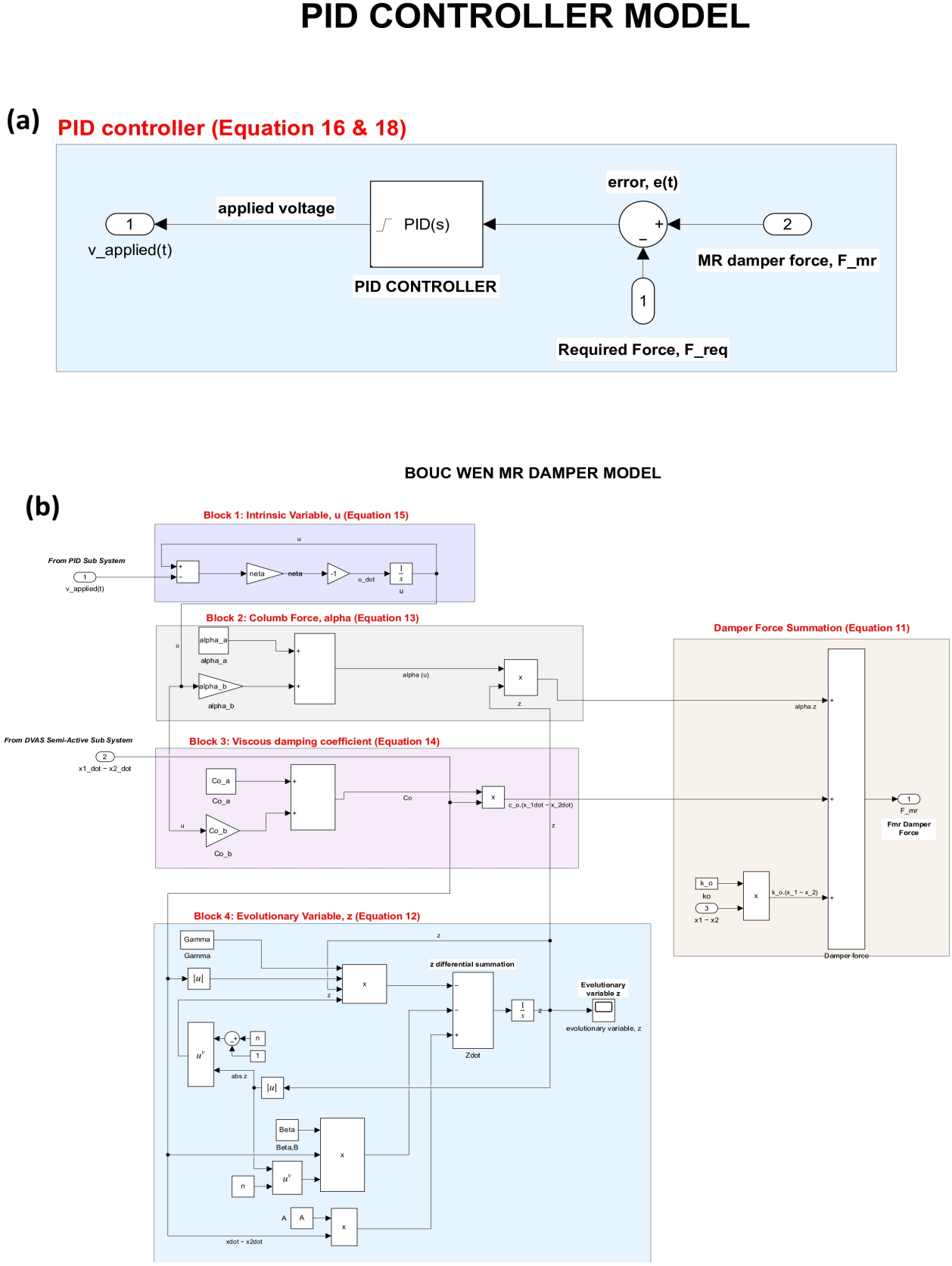

Figure 13. (**a**) Simulink model of PID controller subsystem (**b**) Simulink model of Bouc-Wen MR Damper subsystem.

Table 3. Parameters used in the Bouc-Wen MR damper model, based on [26].

Parameter	Value
A	15
β	1×10^6 m^{-2}
γ	1.2×10^6 m^{-2}
n	2
x_0	0 m
α_b	49,616 Nm^{-1}
η	190 s^{-1}
k_0	300 Nm^{-1}
c_{0a}	4400 Ns·m^{-1}
c_{0b}	442 Ns·V^{-1}m^{-1}
α_a	10,872 Nm^{-1}

3. Results and Discussion

3.1. PID-Controller Tuning of DVAS Semi-Active Suspension

In order to fulfil the suspension performance criteria outlined in Section 2.1, the PID controller of the DVAS IWM-SASS required tuning, which is the process of selecting appropriate values for each of the three gains (K_P, K_i and K_d) of the controller. The trial and error tuning method was used, wherein the gain values were adjusted manually until the desired system response was achieved. Due to the fact that the DVAS semi-active suspension was a complex, non-linear system, the trial and error offered a simple and easy approach to tuning which involved no mathematical formulation, and it is often used by control engineers in industry, as described by [27]. However, it should be noted that the controller gains were still selected based on an understanding of the general effects that each gain value has on the closed-loop response, which is well documented in the literature.

In the final DVAS semi-active suspension model, only a PI controller was required where the proportional gain, K_P, was the main controller parameter utilised since it amplified and scaled the error signal in order to produce a control voltage which could effectively drive the MR damper. Also, the integral gain, K_i, was then used to stabilise the system response and offset the effect of using a higher K_P value. The derivate gain, K_d, was unable to provide any significant improvements across the various system response plots in terms of achieving the suspension performance criteria. Table 4 below summarises the tuned controller parameters of the DVAS semi-active suspension system.

Table 4. Parameters of tuned PID controller of DVAS IWM-SASS and untuned PID controller.

Controller Parameter	Tuned Value	Untuned Value
K_P	10	1
K_i	3	0
K_d	0	0
Applied Voltage Upper limit	+5 V	-
Applied Voltage Lower Limit	0 V	-

Furthermore, saturation was applied to the control output (i.e., applied voltage, v) of the PI controller wherein a upper and lower saturation limit of +5 V and 0 V were specified, respectively. These voltage limits were typical power requirements for an MR damper, and in this case, the upper applied voltage limit was based on [28], whilst the lower limit of 0 V represented the operation of the Bouc-Wen MR damper in passive mode where no energy (or input voltage) was applied.

Figure 14 then highlights the time variation in the control input (error), control output from the PID controller (applied voltage) as well as the resulting Bouc-Wen MR damper force for each of the three road profiles tested. It can be seen that under the action of the PI controller of the DVAS IWM-SASS, the control input (error) was converted into an appropriately scaled voltage signal which was then used to drive the MR damper, for each of the three different road profiles. It can be seen that the applied voltage control output was kept within the limit of 0–5 V due to saturation, as discussed previously. The controllable Bouc-Wen MR damper force is also highlighted in Figure 14, which was produced as a result of the applied voltage and the system response to the respective road profile input. It was further observed that the Bouc-Wen MR damper force followed the same general trend/shape as the control input (error) but was simply rescaled.

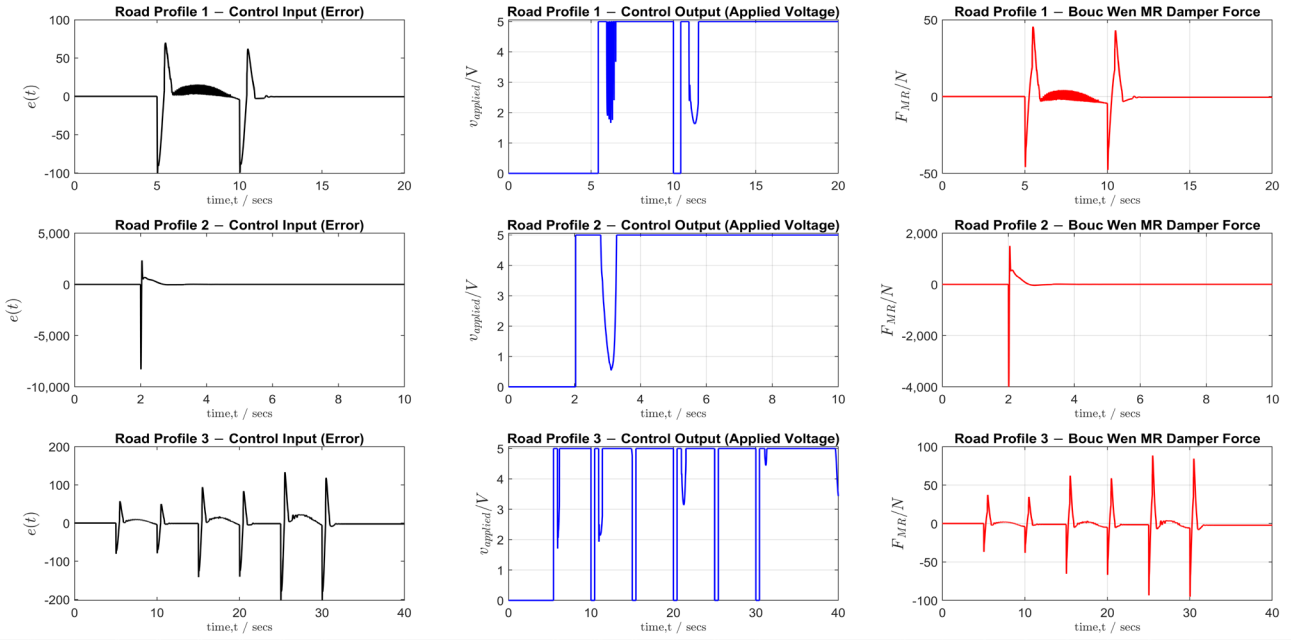

Figure 14. Comparison of the control input (error), control output (applied voltage) and MR damper force of the DVAS semi-active suspension under each of the three road profile inputs.

3.2. DVAS Semi-Active Suspension Parameter Tuning

Apart from PID-controller tuning, the final optimised DVAS semi-active suspension required adjustment of the quarter car model parameters from the original reference values (Table 2). Certain parameters of the Bouc-Wen model were also further optimised over the original reference values that were presented earlier in Table 3. A comparison of the original reference value and optimised values of the system parameters of the DVAS semi-active suspension are shown in Table 5. Firstly, regarding the quarter car model parameters, the DVAS semi-active suspension required greater compliance after introduction of the controllable Bouc-Wen MR damper model, in order to realise an improvement in system response. The increased suspension compliance was achieved by a considerable decrease in the values of spring constants, k_1, k_d and k_b by a decrease in the damping coefficient, b_d. The exact optimised values seen in Table 5 were obtained via trial and error until the desired system performance was achieved across all the response plots which were analysed. Furthermore, regarding the Bouc-Wen MR damper model, the two constants, c_{0a} and c_{0b}, are directly voltage-dependent and influence the overall viscous damping coefficient, c_0, of the MR damper and significantly affect the dynamic force range of the MR damper. The DVAS semi-active suspension was able to produce significantly greater ride comfort (lower sprung mass acceleration) and reduced motor vibration (lower stator

acceleration) by decreasing the effective force range of the Bouc-Wen MR damper, which was carried out by lowering the values of c_{0a} and c_{0b} over the original reference values.

Table 5. System parameters of the final DVAS semi-active suspension which were altered from the original reference values based on [5,26,28] to the optimised values which produced an improved system response performance with PID control.

System Parameter	Original Reference Value	Optimised Value
k_1	28,500 N/m	13,000 N/m
b_d	1900 Ns/m	1200 Ns/m
k_d	53,000 N/m	25,000 Ns/m
k_b	1.4×10^7 N/m	7×10^6 N/m
c_{0a}	4400 Ns·m^{-1}	1300 Ns·m^{-1}
c_{0b}	442 Ns·V^{-1}m^{-1}	350 Ns·V^{-1}m^{-1}

3.3. Suspension System Response

In Figures 13–16, the various system responses of the final tuned DVAS semi-active suspension, DVAS passive suspension and conventional passive suspension were compared for each of the three different road profile inputs. The following should be noted in regard to the comparison response plots:

11. CON IWM-PSS represents the conventional in-wheel motor passive suspension system, as detailed in Figures 4 and 5.
12. DVAS IWM-PSS represents the in-wheel motor passive suspension system with dynamic vibration-absorbing structure, as detailed in Figures 6 and 7.
13. DVAS IWM-PSS (BW) represents the in-wheel motor semi-active suspension system with dynamic vibration-absorbing structure and a constant zero (0) voltage Bouc-Wen MR damper model. This represented the scenario when DVAS IWM-SASS was operating in the fail-safe passive mode with no energy input (0 V) to the damper. Also, the DVAS IWM-PSS (BW) provided a benchmark in order to clearly visualise the performance improvements when feedback control of the voltage-dependent MR damper was then introduced with the DVAS IWM-SASS (BW).
14. DVAS IWM-SASS (BW) represents the in-wheel motor semi-active suspension system with dynamic vibration-absorbing structure and a PID-controlled voltage-dependent Bouc-Wen MR damper, as detailed in Figures 8–10.

As outlined previously, the design goal for the DVAS semi-active suspension was to simultaneously minimise sprung mass acceleration, sprung mass displacement, stator acceleration and tyre deflection whilst also considering suspension travel limits. The comparison response plots for road profiles 1 and 3 were quite similar since road profile 1 was a 0.1 Hz single sine bump, while road profile 3 had three (3) consecutive 0.1 Hz sine bumps of increasing amplitude (i.e., a variation in road profile 1). As such, the response plots for road profiles 1 and 3 were analysed together.

Figure 15 compared the sprung mass acceleration response of the various IWM suspension systems for the three different road profiles tested. For road profile 1, it can be seen that the DVAS passive suspension had a slightly lower peak overshoot amplitude compared to the conventional passive (16% reduction), whilst the undershoot peak amplitude and settling time remained largely unchanged. The DVAS semi-active suspension displayed the greatest performance for road profile 1 with a noticeable 40% reduction in peak overshoot amplitude and a slightly lower peak undershoot amplitude (22% reduction) over the DVAS passive suspension whilst settling time remained unchanged. Meanwhile, the DVAS semi-active suspension (passive fail-safe mode) had a near identical peak overshoot amplitude compared to the DVAS semi-active suspension but with a slightly greater

(19%) peak undershoot. Furthermore, the DVAS semi-active suspension (passive fail-safe mode) had a greater settling time of 12.8 s compared to 11.5 s for the DVAS semi-active and DVAS passive.

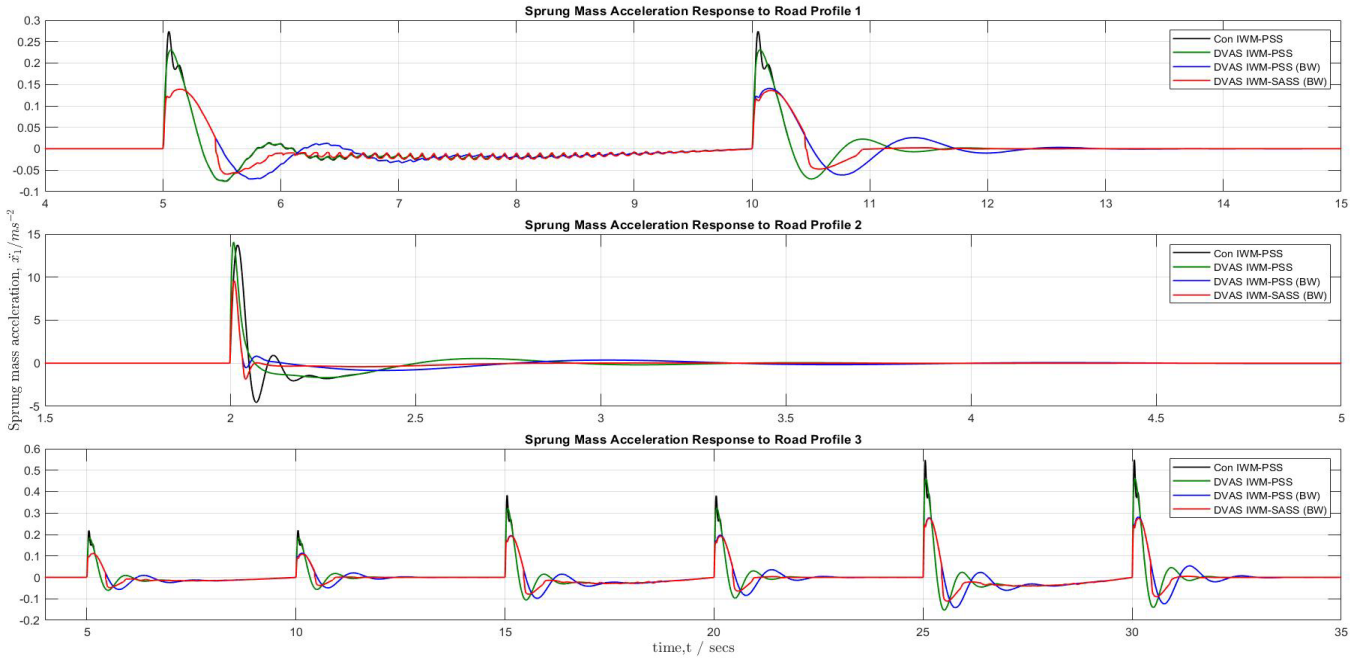

Figure 15. Sprung mass acceleration response of the various IWM suspension systems for each of the three (3) different road profile inputs.

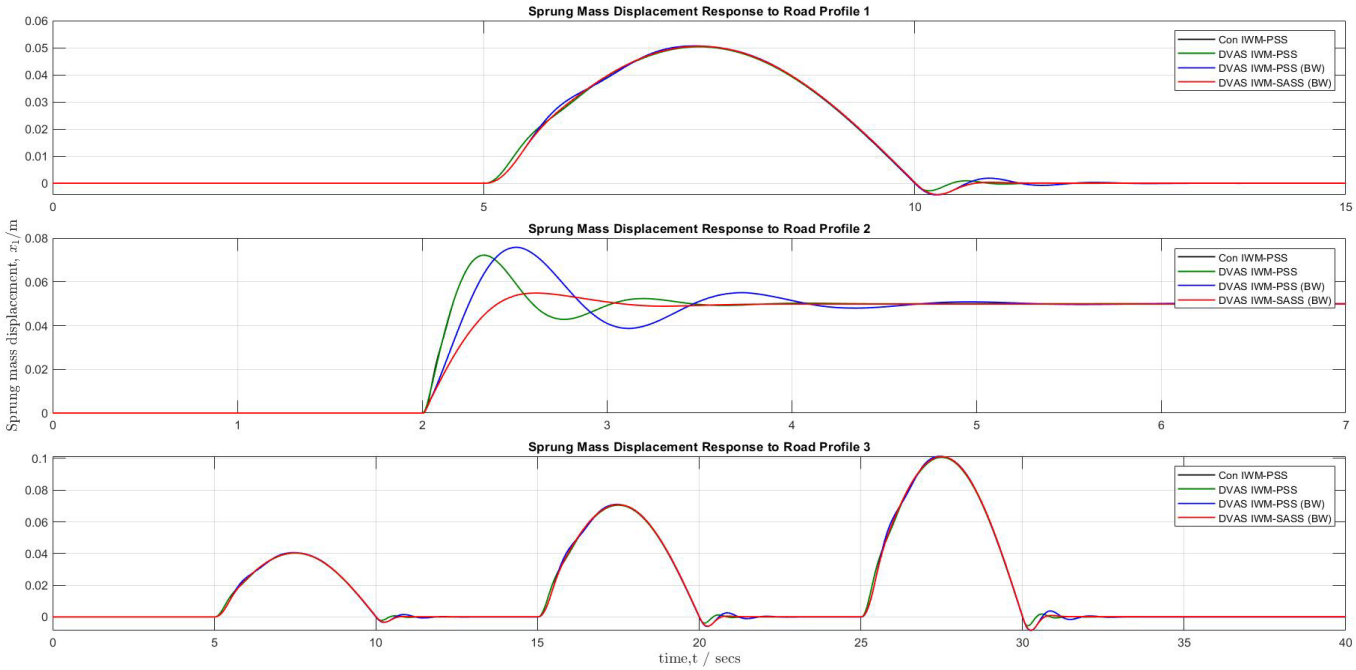

Figure 16. Sprung mass displacement response of the various IWM suspension systems for each of the three (3) different road profile inputs.

For road profile 3, a similar trend was observed as with road profile 1, where the DVAS passive suspension offered slight performance improvements over the conventional passive mainly in terms of peak overshoot amplitude (16% reduction). Again, the DVAS semi-active suspension provided a substantial reduction in peak overshoot amplitude (50% reduction) and a small reduction in peak undershoot amplitude of around 27%

over the DVAS passive suspension. In passive fail-safe mode, the DVAS semi-active had comparable but slightly larger peak amplitudes (similar to the trend of road profile 1) and settling time was increased by approximately 5% over the PID-controlled DVAS semi-active.

In regard to road profile 2, it was observed that the DVAS passive suspension had similar values of peak overshoot amplitude and settling time as compared to the conventional passive, and thus, the DVAS passive suspension was unable to offer any substantial improvements in this regard. However, a noticeable improvement in the peak undershoot amplitude was noted, where the DVAS passive exhibited a considerable 63% reduction over the conventional passive suspension. Regarding the DVAS semi-active suspension, a noticeable 32% and 17% reduction in peak overshoot amplitude and settling time were noted, respectively, over the DVAS passive. However, peak undershoot amplitude was slightly increased by around 12% over the DVAS passive. Furthermore, the performance comparison between the DVAS semi-active in full operation and in passive fail-safe mode produced mixed outcomes where both systems had identical peak overshoot amplitudes, but the semi-active suspension in full operation had a 30% reduction in settling time whilst having a peak undershoot amplitude, which was around 1.2 times greater compared to the passive fail-safe mode.

In Figure 16, it can be seen that for road profiles 1 and 3, the overall response was quite similar for all the IWM suspension systems, particularly in terms of peak overshoot amplitude and general shape/trend of the response. Specifically, the DVAS passive suspension produced an identical response to the conventional passive, whilst the DVAS semi-active in both full operation and passive fail-safe mode had similar performance. Notably, the peak undershoot amplitudes of the DVAS semi-active in full operation and in the passive fail-safe mode were near identical and were increased by around 53% over the DVAS passive and conventional passive, for both road profiles 1 and 3. To add, the settling time of the DVAS semi-active in fail-safe mode was increased compared to all other suspension systems by approximately 9% and 3% for road profiles 1 and 3, respectively.

Furthermore, regarding road profile 2, it can be seen that the conventional passive, DVAS passive and DVAS semi-active in the fail-safe mode all produced quite similar responses, particularly in terms of peak amplitudes. However, it was observed that the response of the DVAS semi-active in the fail-safe mode had the most oscillatory behaviour amongst all four (4) suspension systems which was reflected in the settling time of 5.16 s (highest of all suspension systems tested). The greatest performance was seen with the DVAS semi-active suspension, which produced a response with the least oscillation and variation compared to all the other IWM suspension systems. Numerically, the DVAS semi-active reduced the peak overshoot and undershoot amplitude by approximately 28% and 16% over the DVAS passive. Also, settling time of the DVAS semi-active was lowered by about 5% and 31% over the DVAS passive and DVAS semi-active in the passive fail-safe mode, respectively.

Figure 17 highlights the stator acceleration response of all the DVAS-based IWM suspension systems for each of the three different road profiles. It should be noted that the conventional passive suspension was not included in the comparison response plots of Figure 17, since this setup did not have a separately sprung IWM stator mass and hence would not be a direct comparison to the DVAS-based suspension systems. Firstly, for road profile 1, it can be seen that in terms of peak overshoot amplitude, semi-active suspension in full operation and in passive fail-safe had identical overshoot values, which were slightly improved over the DVAS passive (7% reduction). Moreover, in terms of peak undershoot, the DVAS semi-active had the best performance, since its value was around 32% lower than both the DVAS passive and the semi-active suspension in fail-safe mode. Settling time between all three suspension systems remained largely unchanged for road profile 1. Quite

notably, the DVAS semi-active in full operation produced a much smoother (less oscillatory) response compared to the DVAS passive and the fail-safe mode in the time interval between the two peak amplitudes (between 5.5 s and 10 s). However, interestingly, the DVAS semi-active also had random small amplitude spikes of the sprung mass acceleration which occurred at approximately around 5.5 s and 10.5 s. This phenomenon was not observed in the DVAS passive or the DVAS semi-active in fail-safe mode, which therefore suggests that it was a result of the feedback control.

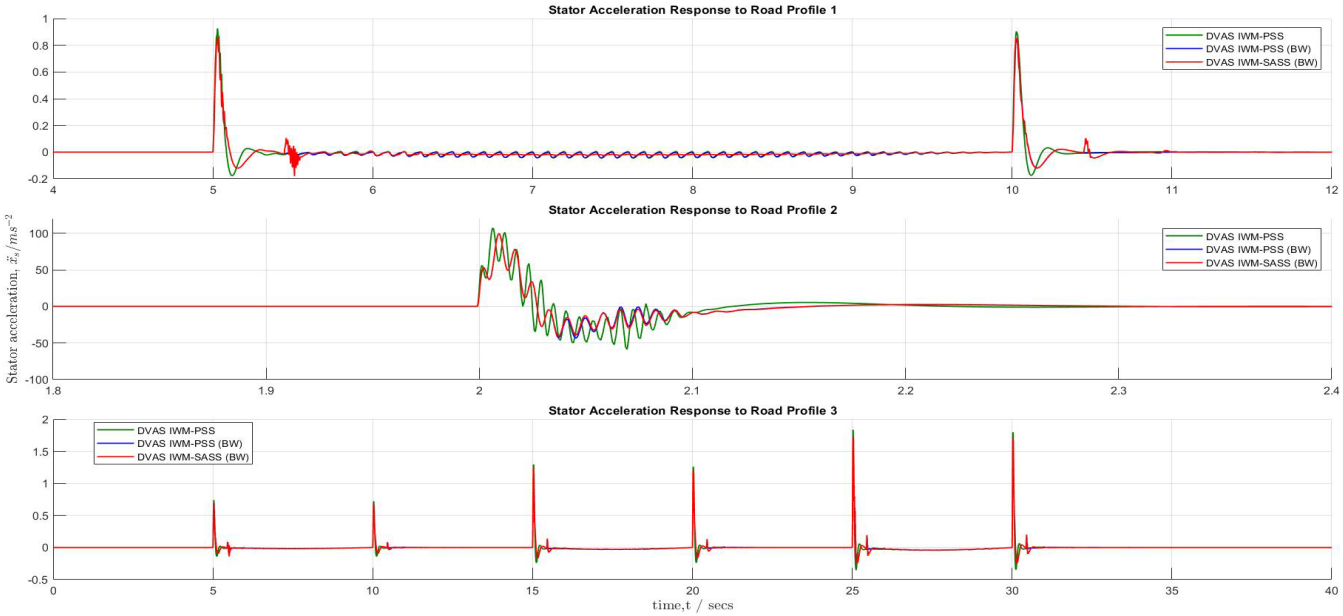

Figure 17. Stator acceleration response of the various IWM suspension systems for each of the three (3) different road profile inputs.

For road profile 3, the trends observed were near enough identical to that of road profile 1 but with slightly different numerical values. Specifically, the DVAS semi-active in full operation and passive fail-safe mode exhibited quite similar responses both in terms of peak overshoot and undershoot amplitude. Numerically, there was an 8% and a considerable 31% reduction in peak overshoot and peak undershoot amplitudes, respectively, of both systems over the DVAS passive suspension. Settling time also remained largely unchanged amongst all three DVAS-based suspension systems for road profile 3 (similar to the trend for road profile 1).

Moreover, regarding road profile 2, it was seen that both the DVAS semi-active in full operation and in fail-safe mode produced a response which had lower amplitudes of the majority of consecutive oscillations, compared to the DVAS passive suspension. Numerically, both the DVAS semi-active in full operation and in fail-safe mode had identical peak overshoot amplitudes, which was slightly lower than that of the DVAS passive suspension by 5%. In terms of peak undershoot, the DVAS semi-active in full operation and in fail-safe mode had comparable values but the DVAS semi-active still displayed the greatest performance in terms of this metric. The peak undershoot of the DVAS semi-active in full operation was around 19% lower than that of the DVAS passive and just 5% lower than that in passive fail-safe mode. Lastly, all three suspension systems had identical settling times for the response to road profile 2.

In Figure 18, the tyre deflection responses of the various IWM suspension systems were compared for each of the three different road profiles. Regarding road profile 1, it was observed that firstly, the DVAS passive suspension had a similar response to the conventional passive but with slight improvements in terms of peak undershoot amplitude, which

was reduced by approximately 16% over the conventional. The DVAS semi-active offered the overall greatest performance in that the peak overshoot and undershoot amplitude was 18% and 24% lower than that of the DVAS passive, respectively. The response of the DVAS semi-active was also overall much less oscillatory but still had the exact settling time as the DVAS passive and conventional passive (11.5 s). Furthermore, the response of the DVAS semi-active in fail-safe mode was quite similar to the full operation performance but had slightly more oscillatory behaviour. This was reflected in the higher settling time of 12.8 s of the DVAS semi-active in fail-safe mode compared to the 11.5 s of all the other IWM suspension systems.

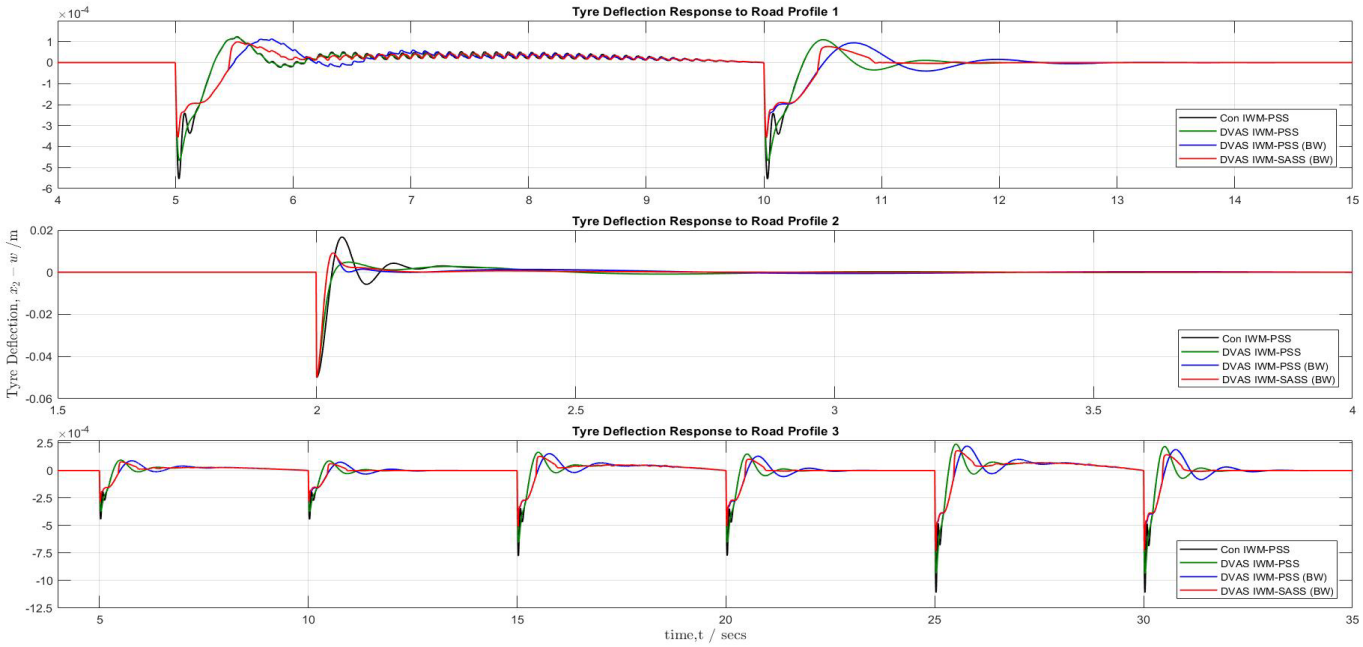

Figure 18. Tyre deflection response of the various IWM suspension systems for each of the three (3) different road profile inputs.

In regard to road profile 3, the same general trends were observed as with road profile 1 but with slightly different numerical values. Again, the DVAS semi-active again offered the greatest overall performance with minimal oscillatory behaviour. The peak overshoot and undershoot amplitude were approximately 25% and 35% lower than that of the DVAS passive.

With respect to road profile 2, all the IWM suspension systems had near identical peak undershoot values. More specifically, when the DVAS passive was compared to the conventional passive suspension, it was noted that the peak overshoot amplitude was considerably reduced by approximately 72% whilst the settling remained unchanged. Notably, the DVAS semi-active was unable to generate any performance improvements over the DVAS passive in terms of peak overshoot amplitude wherein it was observed that the peak overshoot of the DVAS semi-active was actually 92% higher than that of the DVAS passive. However, the overall response of the DVAS semi-active was significantly less oscillatory with lower variation from the final steady state value compared to all the other suspension system responses to road profile 2. It follows that the settling time of the DVAS semi-active was approximately 14% lower than that of both the conventional and DVAS passive. Finally, the DVAS semi-active in passive fail-safe mode was able to produce a near identical response to the full operation apart from the fact that it had a noticeably longer settling time of 3.11 s.

Figure 19 highlights the suspension travel response of the various IWM suspension systems for the different road profiles tested. Regarding road profile 1, it can be seen that the conventional and DVAS passive had a near identical response, which is confirmed by the values of the peak amplitude and settling time. Furthermore, the DVAS semi-active in fail-safe mode displayed the least desirable overall suspension travel performance in that the peak overshoot and undershoot amplitudes were approximately 130% (1.3 times) and 34% greater than that of the DVAS and conventional passive suspensions, respectively. Additionally, the response of the DVAS semi-active in fail-safe mode was much more oscillatory and had a settling time increase of around 11% over the DVAS and conventional passive. Moreover, the DVAS semi-active response in full operation and in fail-safe mode were quite similar particularly in terms of the peak undershoot; however, in full operation, notable improvements in terms of the peak overshoot amplitude was seen (approx. 32% reduction over the DVAS and conventional passive). Furthermore, the settling time of the DVAS semi-active in full operation was comparable with that of the DVAS and conventional passive with minimal oscillations or variations around the equilibrium steady state value.

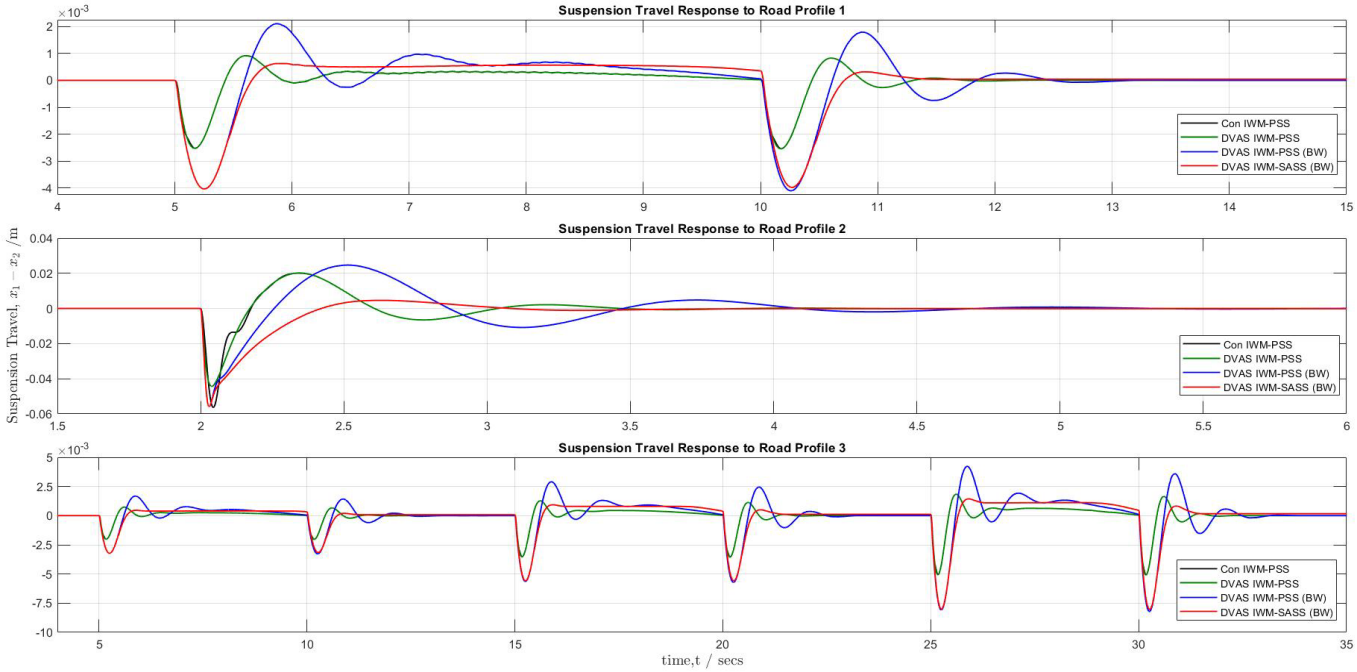

Figure 19. Suspension travel response of the various IWM suspension systems for each of the three (3) different road profile inputs.

For road profile 3, the trends were generally similar to road profile 1 wherein it was noted that the DVAS in full operation and in fail-safe mode increased the peak undershoot amplitude by on average 58% over the DVAS and conventional passive suspensions. Also, the DVAS semi-active in fail-safe mode had the greatest settling time (33.0 s) and largest peak overshoot amplitude amongst all suspension systems at a value of 4.20×10^{-3} m.

With respect to road profile 2, the conventional and DVAS passive suspension had near identical responses apart from the peak undershoot amplitude which was slightly greater (approx. 27%) for the conventional passive. Furthermore, the DVAS semi-active in fail-safe mode was unable to offer any noticeable performance improvements in terms of suspension travel response compared to the DVAS passive and actually had the greatest peak overshoot and undershoot amplitude (0.0247 m and -0.056 m) as well as the longest settling time (5.12 s) compared to all other IWM suspension systems. Regarding the DVAS

semi-active in full operation, the peak undershoot amplitude was similar to the fail-safe; however, the peak overshoot amplitude was nearly eliminated.

4. Conclusions

This paper proposed a semi-active suspension system for in-wheel motors that combined both a dynamic vibration-absorbing structure (DVAS) and a PID-controlled MR damper, in order to achieve optimised comfort, handling and IWM vibration for a small car application. Whilst PID control and DVAS are not entirely new, the usage of both optimisation techniques in a semi-active in-wheel motor suspension has seen limited implementation, which makes the current work novel. Furthermore, unlike other previous work, the semi-active suspension system was tested in full control feedback as well as in passive fail-safe mode. Based on the results of the theoretical and simulated analysis, the following are noted:

- Across all road profiles, the implementation of DVAS by itself offered greater ride comfort and road holding performance over a conventional passive in-wheel motor suspension in terms of peak amplitude reduction in the sprung mass acceleration and tyre deflection, by a maximum of 63% and 72%, respectively, in certain applications.
- The implementation of a PID-controlled MR damper further improved road comfort, road holding performance and decreased in-wheel motor vibration over the DVAS passive suspension mainly in terms of a maximum peak amplitude decrease of 40%, 35% and 32% for the sprung mass acceleration, tyre deflection and stator acceleration, respectively.
- In passive fail-safe mode, the MR damper of the semi-active suspension had a similar but slightly decreased performance to the full operation based on a marginal increase in peak amplitudes and oscillatory behaviour.
- All DVAS-based suspension systems slightly worsened suspension travel compared to a conventional passive in-wheel motor suspension.

In summary, this paper shows that the use of a simple, readily available PID-controlled MR damper (in normal operation and fail-safe mode) together with a dynamic vibration-absorption structure (DVAS) is able to significantly improve comfort, handling and in-wheel motor vibration for a small car application. OEMs should have greater confidence in furthering commercial implementation of the IWM powertrain layout since it has been shown that the issue of increased unsprung mass can be addressed using simple and readily available technology such as a PID controller and an MR damper. Future work will be aimed at improving the PID tuning method by developing a multi-objective weighted function and optimising parameters using Genetic Algorithm (GA). Experimental validation of the DVAS-based semi-active suspension system will be considered, and full/half car models will also be implemented in the extended investigation.

Author Contributions: Conceptualization, K.S.; methodology, K.S. and A.W.A.; software, K.S.; validation, K.S.; data curation, K.S.; writing—original draft preparation, K.S.; writing—review and editing, K.S., A.W.A. and S.I.; supervision, A.W.A. All authors have read and agreed to the published version of the manuscript.

Funding: This research received no external funding.

Data Availability Statement: Research data are readily provided upon request.

Conflicts of Interest: The authors declare no conflicts of interest.

Abbreviations

x_1	sprung (body) mass displacement
x_2	conventional unsprung mass displacement
w	road profile displacement
m_1	sprung (body) mass
m_2	conventional unsprung mass to include IWM (rotor and stator) and all other typical unsprung components
m_{2sc}	unsprung mass excluding IWM (rotor and stator)
m_r	rotor mass of IWM
m_s	stator mass of IWM
k_1	spring constant of passive spring
k_2	spring constant of tyre
k_d	spring constant of DVAS spring
k_b	spring constant of bearing
b_1	damping coefficient of passive damper
b_2	damping coefficient of tyre
b_d	damping coefficient of DVAS damper
F_{MR}	voltage controlled damping force of MR damper
F_{req}	Required damping force of the suspension system
k_0	linear spring stiffness of BW model
c_0	viscous damping coefficient of BW model
A,β,γ,n,x_0	parameters affecting scale and shape of hysteresis loop of MR damper at 0 applied voltage
η	time response of the MR damper
u	intrinsic variable that determines function dependence of parameters on the applied voltage, v
α	Voltage-dependent columb force of MR damper
$v_{applied}$	voltage applied to the MR damper

References

1. United Nations. Paris Declaration on Electro-Mobility and Climate Change & Call to Action. In *Lima-Paris Action Agenda*; UNFCCC: New York, NY, USA, 2015.
2. Sachs, C.; Burandt, S.; Mandelj, S.; Mutter, R. Assessing the market of light electric vehicles as a potential application for electric in-wheel drives. In Proceedings of the 2016 6th International Electric Drives Production Conference (EDPC), Nuremberg, Germany, 30 November–1 December 2016; pp. 280–285.
3. Liu, M.; Gu, F.; Zhang, Y. Ride Comfort Optimization of In-Wheel-Motor Electric Vehicles with In-Wheel Vibration Absorbers. *Energies* **2017**, *10*, 1647. [CrossRef]
4. Fraser, A. *IN-WHEEL ELECTRIC MOTORS*; The Packaging and Integration Challenges; Protean Electric Ltd.: Farnham, UK, 2018.
5. Xu, B.; Xiang, C.; Qin, Y.; Ding, P.; Dong, M. Semi-Active Vibration Control for in-Wheel Switched Reluctance Motor Driven Electric Vehicle With Dynamic Vibration Absorbing Structures: Concept and Validation. *IEEE Access* **2018**, *6*, 60274–60285. [CrossRef]
6. Kulkarni, A.; Sagheer, A.R.; Kapoor, A. A quarter-car suspension model for dynamic evaluations of an in-wheel electric vehicle. *Proc. Inst. Mech. Eng. Part D J. Automob. Eng.* **2018**, *232*, 1139–1148. [CrossRef]
7. Jin, L.; Yu, Y.; Fu, Y. Study on the ride comfort of vehicles driven by in-wheel motors. *Adv. Mech. Eng.* **2016**, *8*, 1687814016633622. [CrossRef]
8. Anderson, M.; Harty, D. Unsprung Mass with In-Wheel Motors-Myths and Realities. *AVEC* **2010**, *10*, 261–266.
9. Deepak, K.; Frikha, M.A.; Benômar, Y.; El Baghdadi, M.; Hegazy, O. In-Wheel Motor Drive Systems for Electric Vehicles: State of the Art, Challenges, and Future Trends. *Energies* **2023**, *16*, 3121. [CrossRef]
10. Kulkarni, A.; Ranjha, S.A.; Kapoor, A. Fatigue analysis of a suspension for an in-wheel electric vehicle. *Eng. Fail. Anal.* **2016**, *68*, 150–158. [CrossRef]
11. Kulkarni, A.; Kapoor, A. Rim and tyre investigation for the in-wheel motor of an electric vehicle using simulations. In Proceedings of the 20th International Congress on Modelling and Simulation, Adelaide, Australia, 1–6 December 2013.

12. Soliman, A.; Kaldas, M. Semi-active suspension systems from research to mass-market—A review. *J. Low Freq. Noise Vib. Act. Control.* **2021**, *40*, 1005–1023. [CrossRef]
13. Metered, H.A. Modelling and Control of Magnetorheological Dampers for Vehicle Suspension Systems. Ph.D. Dissertation, University of Manchester, Manchester, UK, 2010.
14. Choi, Y.-T.; Wereley, N.M. Comparative Analysis of the Time Response of Electrorheological and Magnetorheological Dampers Using Nondimensional Parameters. *J. Intell. Mater. Syst. Struct.* **2002**, *13*, 443–451. [CrossRef]
15. Yao, G.Z.; Yap, F.F.; Chen, G.; Li, W.H.; Yeo, S.H. MR damper and its application for semi-active control of vehicle suspension system. *Mechatronics* **2002**, *12*, 963–973. [CrossRef]
16. Sun, W.; Gao, H.; Yao, B. Adaptive Robust Vibration Control of Full-Car Active Suspensions With Electrohydraulic Actuators. *IEEE Trans. Control. Syst. Technol.* **2013**, *21*, 2417–2422. [CrossRef]
17. Agharkakli, A.; Sabet, G.S.; Barouz, A. Simulation and Analysis of Passive and Active Suspension System Using Quarter Car Model for Different Road Profile. *Int. J. Eng. Trends Technol.* **2012**, *3*, 636–644.
18. Rashid, M.M.; Hussain, M.A.; Rahim, N.A.; Momoh, J.S. Development of A Semi-Active Car Suspension Control System Using Magneto-Rheological Damper Model. *Int. J. Mech. Mater. Eng. (IJMME)* **2007**, *2*, 93–108.
19. Qin, Y.; He, C.; Shao, X.; Du, H.; Xiang, C.; Dong, M. Vibration mitigation for in-wheel switched reluctance motor driven electric vehicle with dynamic vibration absorbing structures. *J. Sound Vib.* **2018**, *419*, 249–267. [CrossRef]
20. Qin, Y.; He, C.; Ding, P.; Dong, M.; Huang, Y. Suspension hybrid control for in-wheel motor driven electric vehicle with dynamic vibration absorbing structures. *IFAC-PapersOnLine* **2018**, *51*, 973–978. [CrossRef]
21. Zhang, K.; Wu, J.; Zhang, Y. *Semi-Active Control of ISD In-Wheel Motors Suspension with Dynamic Vibration Absorber*; SAE International: Warrendale, PA, USA, 2022. [CrossRef]
22. Tan, D.; Lu, C.; Zhang, X. Dual-loop PID control with PSO algorithm for the active suspension of the electric vehicle driven by in-wheel motor. *J. Vibroeng.* **2016**, *18*, 3915–3929. [CrossRef]
23. Xu, H.; Liu, J.; Luo, T.; Yao, Y.; Lv, C. Model-Based Design of an Active Suspension for the Improvement of In-Wheel Motor Drive Electric Vehicle. *IEEE Access* **2024**, *12*, 45597–45615. [CrossRef]
24. Zurich Instruments. *Principles of PID Controllers*; Zurich Instruments: Zürich, Switzerland, 2023.
25. Gillespie, T.D. *Fundamentals of Vehicle Dynamics*; SAE International: Warrendale, PA, USA, 1992; ISBN 978-156-091-199-9.
26. Eshkabilov, S. Modeling and simulation of non-linear or hysteresis behavior of magneto-rheological dampers in the example of quarter-car model. *Prog. Mach. Syst.* **2016**, *5*, 31–46.
27. Van der Zalm, G.M. *Tuning of PID-Type Controllers*; DCT Rapporten; Technische Universiteit Eindhoven: Eindhoven, The Netherlands, 2004; Volume 2004.054.
28. Eshkabilov, S. Modeling and Simulation of Non-Linear and Hysteresis Behavior of Magneto-Rheological Dampers in the Example of Quarter-Car Model. *Int. J. Theor. Appl. Math* **2017**, *2*, 170–189.